

Enthalpy Barriers for Asymmetric S_N2 Alkyl Cation Transfer Reactions between Neutral and Protonated Alcohols

Travis D. Fridgen* and Terry B. McMahon

Department of Chemistry, University of Waterloo, Waterloo, Ontario, Canada, N2L 3G1

Received: August 22, 2002; In Final Form: October 17, 2002

Enthalpy barriers for gas phase asymmetric alkyl cation transfer reactions between neutral and protonated alcohols in mixed alcohol systems have been calculated by B3LYP, MP2, and G3(MP2) computational methods. As expected, on the basis of the proton affinities of the alcohols, the enthalpy barrier for transfer of the larger alkyl cation is calculated to be lower than that for transfer of the smaller alkyl cation. A linear relationship between the difference in gas basicity (GB) between the alcohols and the enthalpy barrier is observed for the less favorable alkyl cation transfer reactions. The slope of the regression line is 0.55, and the intercept (at $\Delta\text{GB} = 0$) is found to be $-22.5 \text{ kJ mol}^{-1}$, which is extremely close to the enthalpy barriers for symmetric alkyl cation transfer. This relationship is discussed in the context of the Hammett relationship. Experiments conducted on the reaction of protonated ethanol with ^{18}O -labeled methanol established that about 7.8% of the protonated ethyl methyl ether formed was via the less favorable methyl cation transfer. This experimental value agrees well with the 8.5% predicted based upon the calculated difference in energy barriers between ethyl and methyl cation transfer (6.1 kJ mol^{-1}). This work shows that in the gas phase, the protonated ether products in mixed alcohol systems are formed via two competing S_N2 reactions and that the efficiency of the less favorable alkyl cation transfer reaction increases as the difference in proton affinity of the two alcohols decreases.

1. Introduction

Bimolecular nucleophilic substitution (S_N2) reactions (eq 1, where X and Y are halogenic¹) have been thoroughly studied by chemists for many years.



This prototypical aliphatic S_N2 reaction is analogous to the gas phase Williamson ether synthesis if X⁻ in eq 1 is simply an alkoxide ion (eq 2).



In solution, these reactions are quite slow, largely because of the need for solvent reorganization in the activation step, which results in unfavorable entropies of activation and therefore small Arrhenius preexponential factors (A). To estimate the intrinsic structural effects of these reactions, free from solvent effects, it is required that these reactions be studied in the gas phase. Relatively recently, the thermochemistry and kinetics of these reactions have been studied extensively in the gas phase by many different experimental methods such as flowing afterglow-selected ion flow tube (FA-SIFT)², high-pressure mass spectrometry (HPMS)³, kinetic energy spectroscopy,⁴ guided ion beam tandem mass spectrometry,⁵ and a novel technique aimed at measuring rate constants down to quite low temperatures in a supersonic expansion.⁶ These studies have culminated in a large body of thermochemical data on halide/alkyl halide clusters ($[\text{X}-\text{R}\text{Y}]^-$ and $[\text{XR}-\text{Y}]^-$ in Figure 1) and the barriers to their interconversion ($[\text{X}-\text{R}-\text{Y}]^-$ in Figure 1).

* To whom correspondence should be addressed. E-mail: tdfrideg@sciborg.uwaterloo.ca.

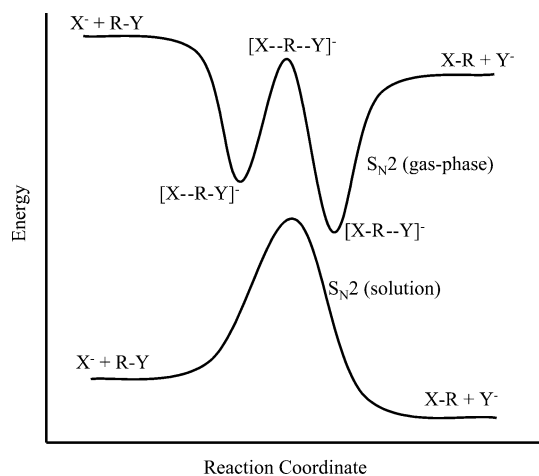


Figure 1. Schematic energy profile for gas phase and solution S_N2 reactions.

An equally significant amount of theoretical work has been published on these reactions. Statistical theories^{7–9} have been widely used to model the kinetics of S_N2 reactions with much success. Hase and co-workers have also undertaken trajectory simulations,^{9–12} which have been useful for interpreting the kinetics and dynamics of S_N2 reactions and have identified shortcomings in some of the assumptions of statistical models.^{10,11} These trajectory studies require accurate potential energy surfaces, the stationary points of which are usually determined by ab initio methods. A very recent study¹³ identified the MP2/6-31+G* level of theory as being quite adequate in describing the energies of the potential energy surface for the S_N2 reaction between hydroxide and methyl fluoride. The central barrier for this reaction was found to be $-21.1 \text{ kJ mol}^{-1}$ with respect to

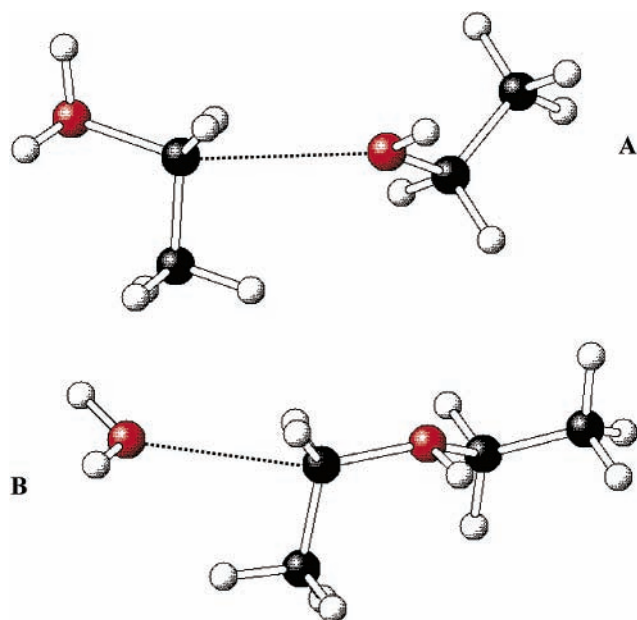


Figure 2. Structures of the protonated ethanol/neutral ethanol complex preceding ethyl cation transfer (A) and the complex between water and protonated diethyl ether following ethyl cation transfer (B).

reactants using the MP2/6-31+G* level of theory, which was only 4.7 or 8.5 kJ mol⁻¹ lower than the values determined using CCSD(T) theory in conjunction with the larger basis sets 6-311++G(2df,2pd) and aug-cc-pVTZ, respectively.

More recently, there have been a number of experimental studies aimed at determining barrier heights for gas phase S_N2 reactions involving alkyl cation transfer such as those in eqs 3 and 4.^{14–20}



Common to all of these gas phase S_N2 reactions involving alkyl cation transfers is the fact that prior to dehydration, the ion/molecule complex must attain a structure in which the oxygen of the neutral alcohol is bound to the α-carbon of the alkyl group of the protonated alcohol (Figure 2A).¹⁵ This “alkyl-bound” complex then undergoes an alkyl cation transfer, effectively from water to the neutral alcohol, producing the water/protonated ether complex (Figure 2B). Because these reactions are so exothermic and the water/protonated ether complexes are so weakly bound, they are not observed in mass spectrometry experiments and only the protonated ether is observed.

One approach to obtaining the energy barriers for the gas phase ion/molecule reactions of eqs 1 and 2 involves measuring rate constants in an ion trap.^{17,18} The rate constants, in combination with Rice–Rampsberger–Kassel–Marcus (RRKM) theory, allow for the estimation of the barrier heights. This method was used to estimate barriers for the reactions between CH₃OH₂⁺ with methanol; CH₃CH₂OH₂⁺ with methanol and ethanol; CH₃CH₂CH₂OH₂⁺ with methanol, ethanol, *n*-propanol, and acetonitrile; (CH₃)₂CHOH₂⁺ with 2-propanol; and CH₃CNH⁺ with methanol and ethanol.

Another purely experimental approach involves measuring the rate constants for the dehydration as a function of temperature within an ion cyclotron resonance (ICR) cell. An Arrhenius analysis of the temperature-dependent rate constants yields purely experimental enthalpies and entropies of activation. This method gives enthalpy barriers that are in much better agreement

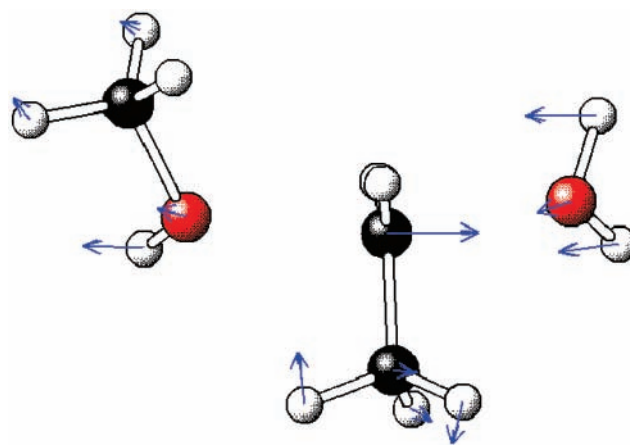


Figure 3. Transition state structure for ethyl cation transfer between protonated ethanol and neutral methanol showing the displacement vectors corresponding to the imaginary vibrational mode.

with values determined computationally.¹⁶ In fact, for the six enthalpy barriers determined experimentally^{15,16} by this method for different methyl, ethyl, and propyl cation transfer reactions, the average difference between the experimental and the calculated (MP2/6-31+G**/B3LYP/6-31+G*, see below) enthalpy barriers is 3.7 ± 2 kJ mol⁻¹ with the calculations always predicting a lower enthalpy barrier than that determined experimentally.

The purpose of this paper is to report on calculated enthalpy barriers for a series of methyl, ethyl, propyl, and butyl cation transfer reactions of the type shown in eq 1, where R ≠ R', producing asymmetric protonated ethers. The method of calculation, described below, is also compared with some higher level calculations, G2(MP2), and experimental values where available. Some experimental results for the reaction of protonated ethanol with neutral methanol are presented, and comparisons are made with the calculated energy barriers.

2. Computational Methods

All calculations were performed using the Gaussian 98²¹ suite of programs. Geometry optimizations and frequency calculations were performed initially using Becke's three parameter hybrid method using the Lee–Yang–Parr correlation functional (B3LYP²²) with the 6-31+G* basis set. This method of calculating the enthalpy barriers is referred to below as B3LYP/6-31+G**/B3LYP/6-31+G*. The B3LYP structures were then optimized using Møller–Plesset perturbation theory truncated at the second order (MP2) in conjunction with the 6-31+G* basis set. The MP2 electronic energies were corrected for thermal contributions to the enthalpy using the B3LYP/6-31+G* frequency calculations. This method of calculating enthalpy barriers, using MP2 electronic energies and B3LYP thermal energies, is referred to as MP2/6-31+G**/B3LYP/6-31+G*. For the smaller systems, enthalpy barriers were calculated using the G3(MP2) method²³ to compare with the other methods used.

Transition state structures were characterized by one imaginary vibrational frequency, which corresponded to motion of the alkyl cation between the oxygen atoms of water and the neutral alcohol. In Figure 3, the vectors corresponding to the motion of each of the nuclei for the imaginary frequency in the transition state structure for the transfer of ethyl cation from protonated ethanol to neutral methanol are shown.

3. Results and Discussion

3.1. Transition State Structures. The B3LYP/6-31+G* and MP2/6-31+G* transition state structures for methyl, ethyl,

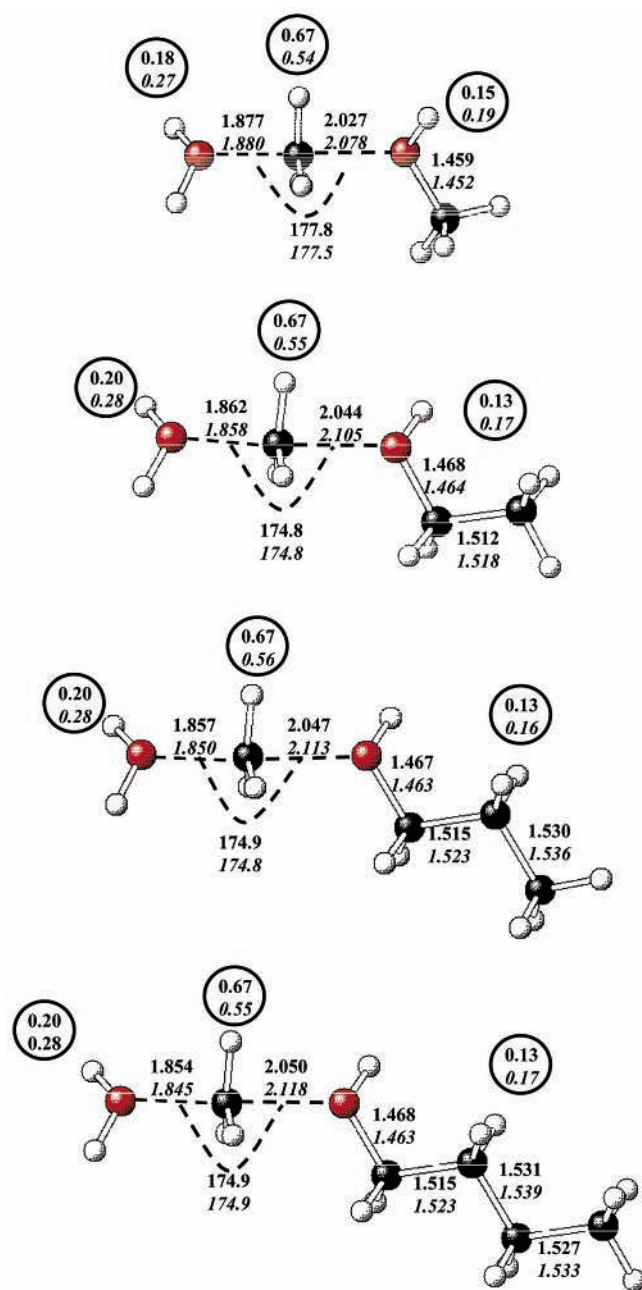


Figure 4. Transition state structures for methyl cation transfer reactions showing bond lengths, angles, and Mulliken charge distributions. Values in plain font are those from the B3LYP/6-31+G* calculations, and italicized values are from MP2/6-31+G* calculations.

propyl, and butyl cation transfer are presented in Figures 4–7, respectively. For the most part, the structures calculated at both levels of theory are in quite good agreement. There is slight disagreement between the two levels of theory in the C–O bond distances between the α -carbon in the transferring alkyl cation and both the water–oxygen (O_w –C) and alcoholic–oxygen (O_a –C). The O_w –C bonds for methyl cation transfer (Figure 4) are quite similar at both methods of calculation whereas the O_a –C bond lengths calculated using MP2 theory range from 0.05 to 0.07 Å longer than those using B3LYP. For ethyl, propyl, and butyl cation transfer, both the O_w –C and the O_a –C bonds are significantly longer at the MP2 level of theory. The longer bonds at the MP2 level of theory imply that the transition states calculated at this level are looser than those calculated at the B3LYP level of theory.

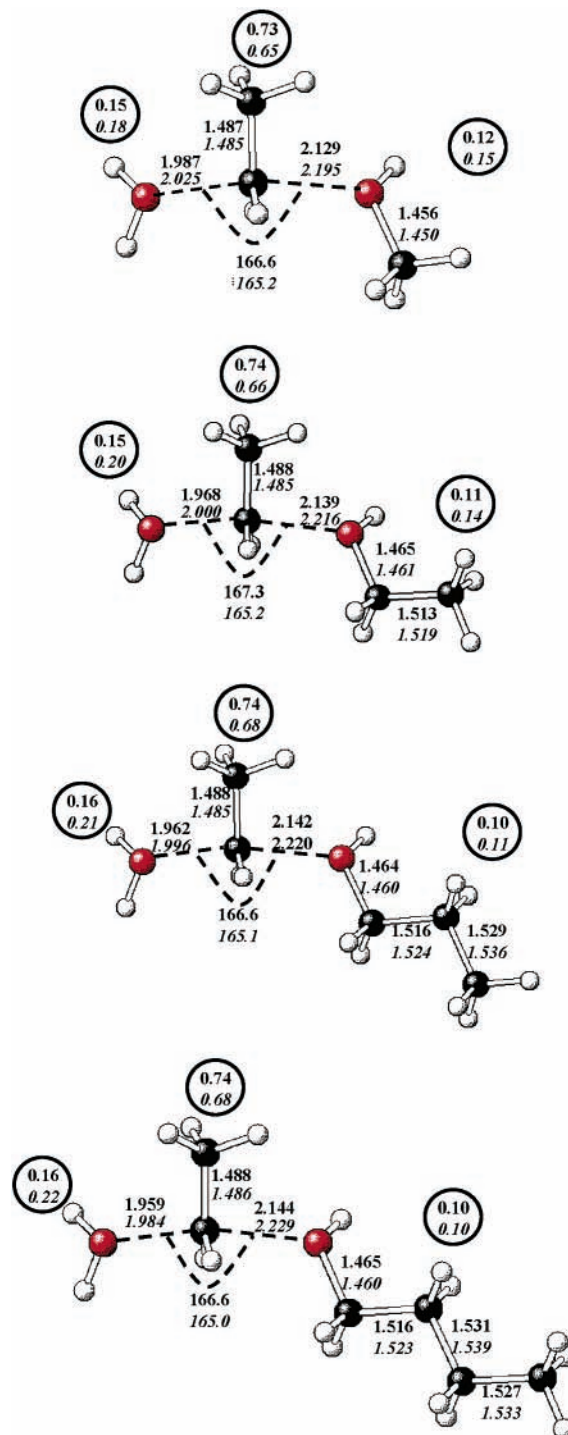


Figure 5. Transition state structures for ethyl cation transfer reactions showing bond lengths, angles, and Mulliken charge distributions. Values in plain font are those from the B3LYP/6-31+G* calculations, and italicized values are from MP2/6-31+G* calculations.

In all cases, the O_w –C bonds are significantly shorter than the O_a –C bonds. For methyl cation transfer, the differences in these bond lengths range from 0.15 to 0.20 Å for the B3LYP calculations and from 0.20 to 0.27 Å for the MP2 calculations and similar differences are observed for the ethyl, propyl, and butyl transfer transition state structures. The C–O bond length in protonated methanol is 1.525 Å at the B3LYP level of theory, which is longer than the C–O bond lengths of protonated dimethyl ether, 1.498 Å. Similarly, for protonated ethanol, the B3LYP C–O bond length is 1.572 Å, and for protonated diethyl ether, they are 1.523 and 1.530 Å,²⁴ again longer for the

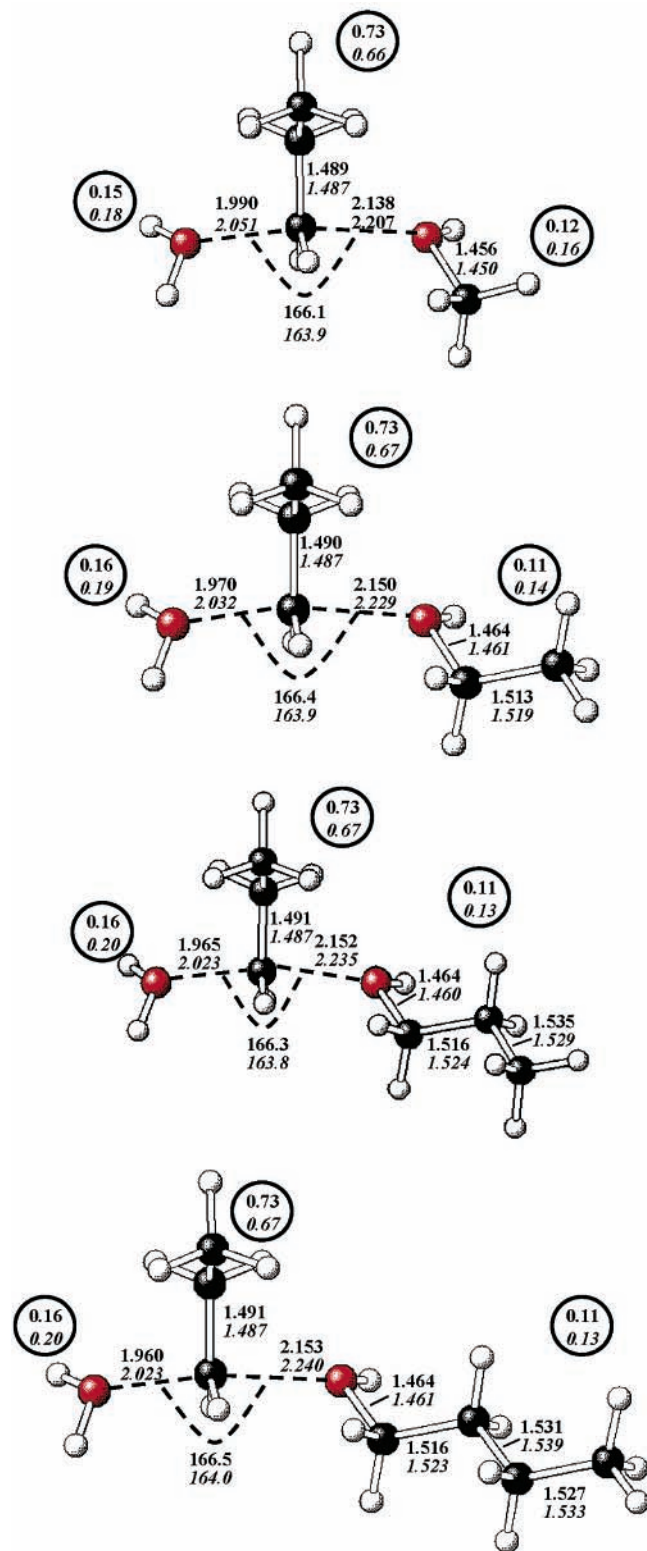


Figure 6. Transition state structures for *n*-propyl cation transfer reactions showing bond lengths, angles, and Mulliken charge distributions. Values in plain font are those from the B3LYP/6-31+G* calculations, and italicized values are from MP2/6-31+G* calculations.

protonated alcohol. The transition state structures, having shorter O_w-C than O_a-C bonds, resemble the reactants more so than products, which is consistent with an early transition state. For each of the methyl, ethyl, propyl, and butyl cation transfer transition states, the difference between the O_w-C and the O_a-C bonds increases as the size of the alcohol or nucleophile increases from methanol to butanol. In fact, in the transition

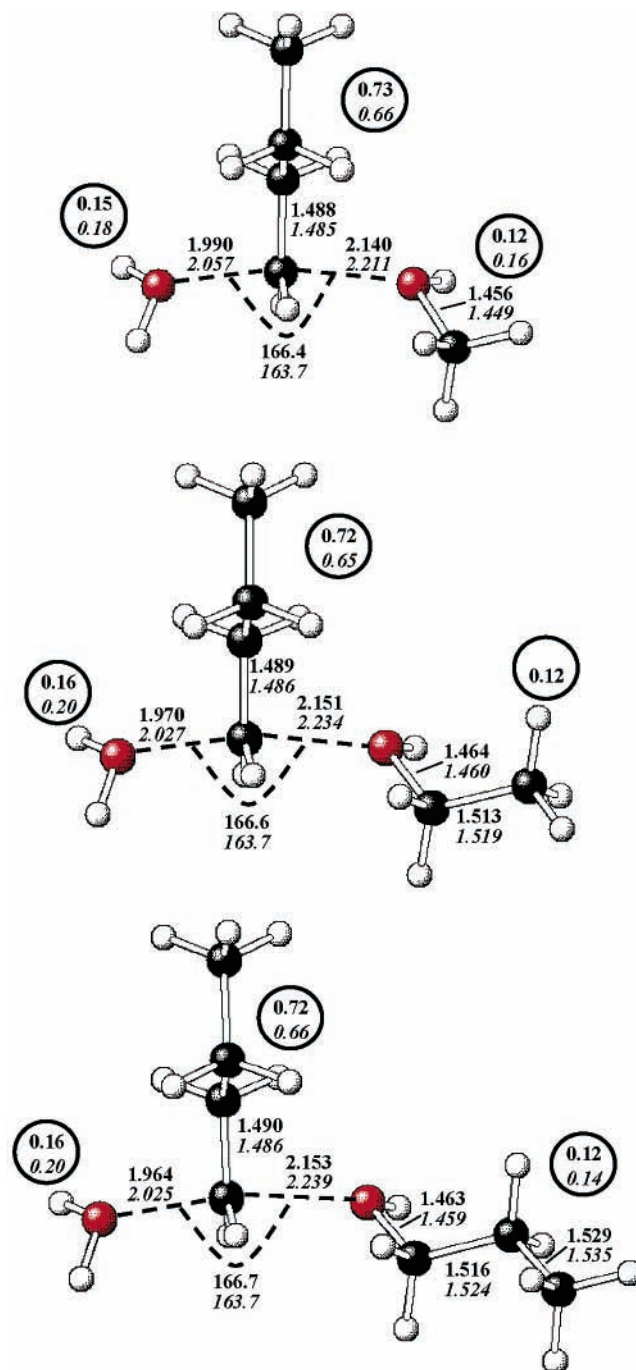


Figure 7. Transition state structures for *n*-butyl cation transfer reactions showing bond lengths, angles, and Mulliken charge distributions. Values in plain font are those from the B3LYP/6-31+G* calculations, and italicized values are from MP2/6-31+G* calculations.

states, the O_w-C bond contracts and the O_a-C bond gets longer suggesting that the transition state is earlier for the heavier nucleophiles.

The charges on the fragments of each of the transition states (water, alkyl group, and alcohol) are also shown in Figures 4–7. The smaller portion of charge on the alcohol than on the water moieties of the transition states, albeit slight, is also indicative of an early transition state.

3.2. Imaginary Vibrational Frequencies. In Table 1 are listed the imaginary vibrational wavenumbers for each of the alkyl cation transfer transition state structures calculated. The motion corresponding to these imaginary frequencies is shown in Figure 3 for the example of ethyl cation transfer from

TABLE 1: Imaginary Vibrational Wavenumbers^a for the Alkyl Cation Transfer Reactions

alkyl cation	transfer to			
	methanol	ethanol	propanol	butanol
methyl	380	373	368	366
ethyl	309	306	306	304
propyl	295	290	290	288
butyl	290	288	285	

^a B3LYP/6-31+G* in units of $i\text{ cm}^{-1}$.

protonated ethanol to methanol. It can be seen from Table 2 that the vibrational wavenumber for the motion in the reaction coordinate does not change appreciably for each alkyl cation transfer. For example, for the methyl cation transfer reactions, the vibrational wavenumber varies only slightly between 366i and 380i cm^{-1} . However, the vibrational wavenumbers are substantially smaller for ethyl, propyl, and butyl cation transfer ranging from 310i to 285i cm^{-1} . The smaller imaginary vibrational frequencies for ethyl, propyl, and butyl cation transfers are primarily due to a substantially smaller force constant in the transition state. The force constants are approximately 0.60 mDyne/A for methyl cation transfer, 0.29 mDyne/A for ethyl cation transfer, and 0.25 mDyne/A for both propyl and butyl cation transfer. The lower force constants are related to the fact that the $\text{O}_w\text{-C}$ and $\text{O}_a\text{-C}$ bonds in the heavier alkyl cation transfer transition state structures are longer than those for the methyl cation transfer transition state structures.

3.3. Barriers for Alkyl Cation Transfer. In Table 2, the energies of the transition states for the various alkyl cation transfer reactions with respect to the lowest energy reactants are listed. For example, the reactants for methyl cation transfer in the methanol/ethanol system are protonated ethanol and neutral methanol even though the transition state for this reaction channel resembles protonated methanol and neutral ethanol.²⁵ These reactants are also the precursors to ethyl cation transfer, and the products of both the methyl and the ethyl cation transfer reactions are protonated ethyl methyl ether (EME) and neutral water. The differences in the enthalpies of activation for these two competing reactions will be discussed in more detail below.

The enthalpy barriers calculated by the three methods of calculation, described above, are compared in Table 2. It is evident that MP2/6-31+G**/B3LYP/6-31+G* enthalpy barriers

are in good agreement with those calculated using G3(MP2) theory and are on average lower by $2.5 \pm 3.4\text{ kJ mol}^{-1}$. More importantly, these values are also in good agreement with those experimental values determined by us^{15,16} being lower on average by $3.7 \pm 2.2\text{ kJ mol}^{-1}$. This lends confidence to the predictive value of the MP2/6-31+G**/B3LYP/6-31+G* calculated enthalpies of activation for the mixed alkyl cation transfer reactions.

By comparing the calculated enthalpies of activation for the two possible reactions between any set of reactants, it can be seen that for all cases, the alkyl cation transfer involving the larger alkyl cation is more favorable than transfer of the smaller alkyl cation. For example, the enthalpy of activation for methyl cation transfer between protonated ethanol and neutral methanol is found to lie 8.7 kJ mol^{-1} below reactants whereas the barrier to ethyl cation transfer between the same two reactants lies lower in energy at 14.8 kJ mol^{-1} below the energy of the reactants. The methyl cation transfer reaction is preceded by a transfer of the proton to methanol from protonated ethanol and formation of an alkyl-bound complex, which has been discussed previously.^{15,26,27} The alkyl-bound complexes have been shown computationally to lie in a quite shallow well with an isomerization barrier (to and from the proton-bound dimer), which is substantially lower in energy (ca. 25–30 kJ mol^{-1}) than the $\text{S}_{\text{N}}2$ barrier.^{15,26,27} The proton transfer to methanol from protonated ethanol in the activated complex prior to methyl cation transfer would result in a much higher energy complex since the proton affinity of methanol is lower than that of ethanol and also results in a higher enthalpy of activation for methyl cation transfer vs ethyl cation transfer. In fact, our calculations show that the isomer preceding methyl cation transfer lies 30.6 kJ mol^{-1} lower in energy than the reactants, protonated ethanol and methanol, (i.e., 21.9 kJ mol^{-1} lower in energy than the methyl cation transfer transition state), and the isomer preceding ethyl cation transfer lies 45.4 kJ mol^{-1} lower in energy than the reactants (30.6 kJ mol^{-1} lower in energy than the ethyl cation transfer transition state).

By comparing the enthalpies of activation in Table 2, it can be seen that the largest difference in enthalpies of activation for two competing alkyl cation transfers results from the reaction of protonated butanol and neutral methanol. The transition state for methyl cation transfer between this set of reactants is

TABLE 2: Calculated and Experimental Energy Barriers^a for $\text{S}_{\text{N}}2$ Alkyl Cation Transfer Reactions

	calculated enthalpy of activation			experimental enthalpy of activation	
	B3LYP/6-31+G**/ B3LYP/6-31+G*	MP2/6-31+G**/ B3LYP/6-31+G*	G3(MP2)	McCormack and Mayer ^{b,c}	Fridgen and McMahon
methyl cation transfer reactions (reaction with neutral methanol)					
CH_3OH_2^+	-30.0	-22.7	-22.4	1 ± 8	-16.9 ± 0.6^d
$\text{CH}_3\text{CH}_2\text{OH}_2^+$	-9.5	-8.7	-6.5		
$\text{CH}_3\text{CH}_2\text{CH}_2\text{OH}_2^+$	-5.7	-5.0			
$\text{CH}_3(\text{CH}_2)_3\text{OH}_2^+$	-3.0	-3.7			
CH_3CNH^+	-13.9	-17.9	-17.8	13 ± 8 (-6 ± 10) ^c	-16.5 ± 0.6^d
CH_3CHOH^+	-20.7	-23.7	-15.4		-18.4 ± 0.7^d
ethyl cation transfer reactions					
$\text{CH}_3\text{CH}_2\text{OH}_2^+ + \text{CH}_3\text{OH}$	-18.2	-14.8	-13.4	6 ± 8	
$\text{CH}_3\text{CH}_2\text{OH}_2^+ + \text{CH}_3\text{CH}_2\text{OH}$	-23.3	-20.2		-5 ± 8	-16.1 ± 0.8^e
$\text{CH}_3(\text{CH}_2)_2\text{OH}_2^+ + \text{CH}_3\text{CH}_2\text{OH}$	-20.5	-17.6			
$\text{CH}_3(\text{CH}_2)_3\text{OH}_2^+ + \text{CH}_3\text{CH}_2\text{OH}$	-17.7	-15.3			
$\text{CH}_3\text{CH}_2\text{CNH}^+ + \text{CH}_3\text{CH}_2\text{OH}$	-12.9	-18.1			-17.5 ± 0.8^e
<i>n</i> -propyl cation transfer reactions					
$\text{CH}_3(\text{CH}_2)_2\text{OH}_2^+ + \text{CH}_3\text{OH}$	-16.1	-15.7		0 ± 8	
$\text{CH}_3(\text{CH}_2)_2\text{OH}_2^+ + \text{CH}_3\text{CH}_2\text{OH}$	-22.2	-21.3		-8 ± 8	

^a kJ mol^{-1} . ^b Experimental values by a combination of quadrupole ion trap kinetics and RRKM modeling from ref 17 or 18. ^c Value in parentheses from metastable ion unimolecular dissociation kinetics in conjunction with RRKM modeling; ref 20. ^d Ref 15. ^e Ref 16.

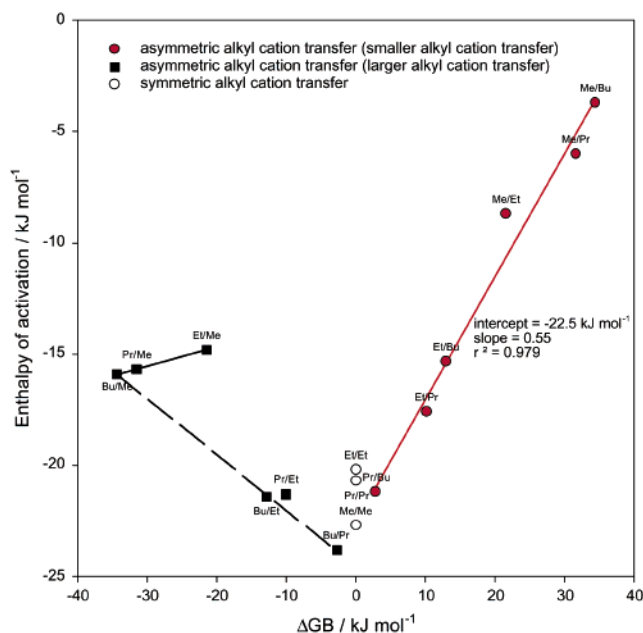


Figure 8. Plot of enthalpies of activation for the various alkyl cation transfer reactions (MP2/6-31+G*/B3LYP/6-31+G*) vs the difference in gas basicities of the pairs of alcohols.

calculated to be -3.7 kJ mol^{-1} with respect to reactants while butyl cation transfer is calculated to be 12.2 kJ mol^{-1} lower in energy ($-15.9 \text{ kJ mol}^{-1}$ with respect to reactants). It should also be noted that butanol and methanol have the largest difference in proton affinity of any set of alcohols studied here. It can also be seen that the competing propyl and butyl cation transfer reactions of protonated butanol and neutral propanol have enthalpies of activation that are the closest of any of the competing alkyl cation transfer reactions differing by only 2.4 kJ mol^{-1} , favoring butyl cation transfer. Butanol and propanol have proton affinities that are the most similar of any of the pairs of alcohols examined. These comparisons reveal a relationship between the calculated enthalpies of activation and the proton affinities of the two alcohols.

3.4. Enthalpies of Activation vs Proton Affinity. In Figure 8, the enthalpy of activation for each of the reactions vs the difference in gas basicity (ΔGB) between the reactant alcohols is plotted. Gas phase basicities were used rather than proton affinities to provide a semblance to the Hammett relationship, which is discussed below. The ΔGB value is calculated by subtracting the GB of the acceptor alcohol (nucleophile) from the GB of the donor alcohol. Therefore, ΔGB for methyl cation transfer between methanol and protonated ethanol is 21.5 kJ mol^{-1} while ΔGB for the more favorable ethyl cation transfer between these reactants is $-21.5 \text{ kJ mol}^{-1}$. Consequently, for values of ΔGB that are greater than zero, the enthalpy of activation for the less favorable alkyl cation transfer reaction between the pair of reactants is plotted. The symbol Et/Bu, in Figure 8, represents an ethyl cation transfer between the reactants protonated butanol and neutral ethanol, while Bu/Et represents butyl cation transfer between the same set of reactants.²⁵

It is readily apparent from Figure 8 that there is a convincing linear relationship between the enthalpy of activation and the ΔGB for all of the reactions involving the least favorable alkyl cation transfer reaction between two pairs of reactants (red circles in Figure 8). The slope of the regression line (red) is 0.55, and the intercept is $-22.5 \text{ kJ mol}^{-1}$, which is similar to the enthalpy barriers for the three symmetric alkyl cation transfer reactions, which have an average of $-21.2 \text{ kJ mol}^{-1}$. This could suggest that the barriers for symmetric alkyl cation transfer in

the gas phase are similar. In fact, the experimentally determined enthalpy barriers for the symmetric methyl,¹⁵ ethyl,¹⁶ and propyl¹⁶ cation transfer reactions are actually quite similar, -16.9 ± 0.6 , -16.1 ± 0.8 , and $-15.7 \pm 0.9 \text{ kJ mol}^{-1}$, respectively.

There are two other regression lines given in black in Figure 8, which concern transfer of the heavier alkyl group or the more favored alkyl cation transfer reaction between two sets of alcohols. We also realize that each of the two regression lines are for only three different reactions. The first (solid line) is for ethyl, propyl, and butyl cation transfers to neutral methanol from the corresponding protonated alcohols. It is apparent that as the alkyl cation being transferred gets larger, over this series, the lower is the activation energy barrier. This may reflect a growing stability of either the complex preceding or the complex following alkyl cation transfer (like A or B, respectively, in Figure 2), which would have the effect of decreasing the energy barrier separating the two complexes. The second (dashed line) is for butyl cation transfer from protonated butanol to neutral methanol, ethanol, and propanol. In this case, nucleophilic alcohol is increasing in size and as it does, a decrease in the energy barrier is observed. Once again, the stability of the complexes preceding and/or following alkyl cation transfer may increase, which has the effect of decreasing the energy barrier separating the two.

As suggested above, the relationship between the enthalpy of activation and the difference in gas phase basicity, depicted in Figure 8, is reminiscent of the solution phase Hammett relationship, given in eq 5.

$$\ln \frac{k}{k_{\text{ref}}} \propto \ln \frac{K}{K_{\text{ref}}} \quad (5)$$

The Hammett relationship was originally recognized for hydrolysis reactions of substituted benzoic acids. Therefore, k and k_{ref} are the rate constants for acid hydrolysis of a substituted benzoic acid and benzoic acid, respectively, and K and K_{ref} are the acid dissociation constants for the substituted benzoic acid and benzoic acid, respectively. The reactions that follow the Hammett equation do so in solution phase, but here, we are dealing with the gas phase. The acid dissociation constants can be compared to the gas phase protonation of base



where M is the base, $\Delta_r G^\circ$ is the Gibbs free energy change associated with the reaction, and GB is called the gas basicity of M. GB, then, can be written in terms of the equilibrium constant

$$-\Delta_r G^\circ = \text{GB} = RT \ln K \quad (7)$$

or

$$K = e^{(\text{GB}/RT)} \quad (8)$$

where R and T are the ideal gas constant and Kelvin temperature, respectively. An equation similar to eq 8 can be written in terms of K_{ref} and GB_{ref}

$$K_{\text{ref}} = e^{(\text{GB}_{\text{ref}}/RT)} \quad (9)$$

Dividing eq 8 by eq 9 yields

$$\frac{K}{K_{\text{ref}}} = \exp(\text{GB} - \text{GB}_{\text{ref}}) \quad (10)$$

Substitution of eq 10 into eq 5 yields

$$\ln \frac{k}{k_{\text{ref}}} \propto \Delta\text{GB} \quad (11)$$

where ΔGB is the difference in GB between two alcohols.

The Arrhenius expression for the rate constant is

$$k = Ae^{-(E_a/RT)} \quad (12)$$

where A is the Arrhenius preexponential factor and E_a is the activation energy. Recently, it has been shown¹⁶ that experimental and theoretical values of the preexponential factor for these alkyl cation transfer reactions are virtually the same because of similar entropies of activation for these reactions. Therefore, assuming that A and A_{ref} are approximately the same

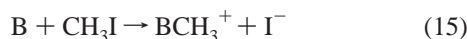
$$\frac{k}{k_{\text{ref}}} \cong \exp(E_{a,\text{ref}} - E_a) \quad (13)$$

so that eq 11 can be rewritten as

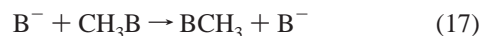
$$\Delta E_a \propto \Delta\text{GB} \quad (14)$$

which shows that the Hammett relationship can simply be regarded as a correlation between the difference in activation energy for two reactions and the difference in GB of the two reactants.

Relationships between energy barriers and proton affinities have been observed previously. Experimental solution phase free energies of activation for the Menshutkin reaction (eq 15, where B is a nitrogen n -donor base) were shown to be linearly related to the gas phase proton affinities ($-\Delta_r H^\circ$ for reaction 6),²⁸ and this relationship was also varified by ab initio calculations.²⁹



Linear relationships of this sort have also been observed for the identity methyl cation transfer reactions of the type



where $A = \text{NH}_3, \text{H}_2\text{O},$ or HF and $B^- = \text{NH}_2^-, \text{OH}^-,$ or F^- and a separate linear relationship for $B^- = \text{I}^-, \text{Br}^-, \text{Cl}^-,$ or F^- .³⁰ Another computational study on neutral base-catalyzed intramolecular proton transfer reactions³¹ made notice of a linear dependence of the magnitude of the decrease in the energy barrier on the difference in proton affinity between the neutral base and the proton leaving site of the substrate. This Hammett-like relationship was shown to be independent of the base or substrate.

It should be noted that each of these reactions, including the alkyl cation transfer reactions, are concerted $\text{S}_{\text{N}}2$ reactions where a bond to the carbon of the transferring alkyl cation is being broken in concert with formation of a new bond. The free energies of activation are expected to be related to the free energy difference between reactants and products (Leffler–Hammond principle).³² For these reactions, the free energy difference between reactants and products is the difference in free energies for methyl cation transfer between the two bases, water and alcohol. Because it has been shown that the methyl cation affinity and proton affinity of various bases are linearly related,^{33,34} the linear relationships depicted in Figure 8 should be of no surprise.

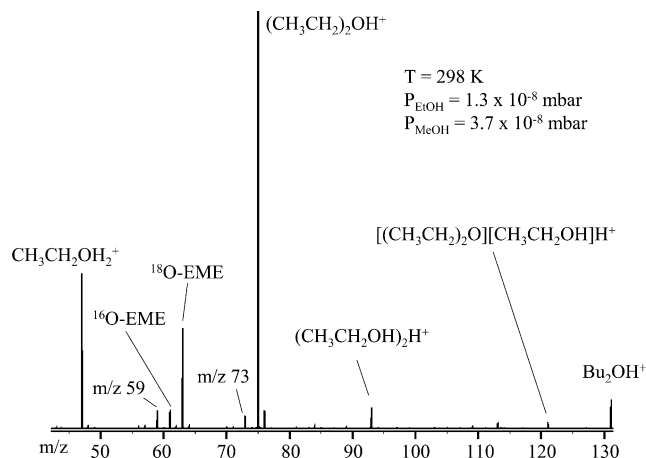


Figure 9. Mass spectrum obtained after 45 s reaction of isolated protonated ethanol with neutral ethanol and neutral methanol ($92.9 \pm 1.1\%$ ^{18}O labeled).

3.5. Ethyl vs Methyl Cation Transfer in the Reaction of EtOH_2^+ With Me^{18}OH . Experiments have been performed in which neutral ^{18}O -labeled methanol was allowed to react with protonated ethanol in the gas phase in an FTICR cell. Such experiments have been described in detail elsewhere.^{14–16} Briefly, vapor from both ethanol and ^{18}O -labeled methanol was leaked into the vacuum chamber housing the FTICR cell. Ions were created with 50 ms pulses of 70 eV electrons. Following the ionization pulse, protonated ethanol was formed by a series of ion/molecule reactions during a short delay (5–10 s). After this delay, all ions except protonated ethanol (m/z 47) were ejected from the ICR cell using standard radio frequency ejection techniques. The isolated protonated ethanol then was allowed to react with the methanol (and ethanol) vapor.

A mass spectrum obtained after 45 s reaction time is shown in Figure 9. The products of protonated ethanol reacting with ethanol are evident at m/z 75 (protonated diethyl ether), m/z 93 (proton-bound dimer of ethanol), m/z 121 (proton-bound dimer of ethanol and diethyl ether),³⁵ and m/z 73, which is a dehydrogenation product of m/z 75.¹⁶ As well, peaks are present due to protonated EME at m/z 61 (^{16}O EME) and 63 (^{18}O EME), which are due to the reaction of protonated ethanol with neutral methanol. There are also peaks at m/z 59 and m/z 131, which are most likely due to acetone and dibutyl ether contaminants present in the methanol in trace amounts. We can rule out that the peak at m/z 59 is due to dehydrogenated EME since we do not observe the ^{18}O isotopomer at m/z 61, which would be resolvable from ^{16}O EME (also at m/z 61) since the two species are separated in mass by 0.012 amu.

Experiments showed that the ^{18}O -labeled methanol contained 7.1 (± 1.1)% methanol- ^{16}O . Therefore, if only ethyl cation transfer was occurring between protonated ethanol and neutral methanol, we would expect to observe 7.1% ^{16}O EME. Our experiments over a number of different pressures of neutral methanol show that there is 14.9 (± 1.5)% ^{16}O EME. Therefore, there is at least roughly 7.8% ^{16}O EME that is due to the less favorable methyl cation transfer from protonated methanol to ethanol following an intramolecular proton transfer from ethanol to methanol. This value agrees remarkably well with what is expected based on the calculated energy barriers. The difference in calculated barriers for ethyl cation transfer and methyl cation transfer is 6.1 kJ mol^{-1} , which would result in an expected 8.5% methyl cation transfer if we assume that the entropy barriers were identical.

These results show that for the reaction of protonated ethanol and neutral methanol both ethyl and methyl cation transfer do

occur. If the difference in energy barriers for the competing reactions is even smaller (i.e., for the reaction of protonated butanol with neutral propanol), then it would be expected that there would be an even larger contribution from the less favorable reaction pathway. For example, on the basis of the calculated energy barriers, protonated butyl propyl ether formed in the reaction between protonated butanol and neutral propanol would be expected to be a product of the less favorable propyl cation transfer about 38% of the time. This would obviously affect the results of the studies by McCormack and Mayer¹⁷ who measured the rate constant for depletion of the protonated precursor for various mixed systems and performed statistical calculations with the energy barrier for alkyl cation transfer as a variable to obtain the barrier.

4. Conclusions

The energy barriers for gas phase alkyl cation transfer reactions between neutral and protonated alcohols in mixed alcohol systems have been studied by computational methods. As expected, on the basis of the proton affinities of the alcohols, transfer of the larger alkyl cation was found to be more facile based on the calculated enthalpy barriers. A linear relationship between the difference in GB between the alcohols and the enthalpy barrier is observed for the less favorable alkyl cation transfer reactions. This relationship was explained in the context of the Hammett relationship.

Experiments conducted on the reaction of protonated ethanol with ¹⁸O-labeled methanol concluded that about 7.8% of the protonated EME formed was via the less favorable methyl cation transfer. This experimental value agrees well with the 8.5% predicted based upon the calculated difference in energy barriers between ethyl and methyl cation transfer (6.1 kJ mol⁻¹). This work shows that in the gas phase, the product protonated ethers in mixed alcohol systems are formed via two competing S_N2 reactions and that the efficiency of the less favorable alkyl cation transfer reaction increases as the difference in proton affinity of the two alcohols decreases.

Acknowledgment. The financial support from the Research Grants Program of the Natural Sciences and Engineering Research Council of Canada (NSERC) as well as from the Americal Chemical Society Petroleum Research Fund is gratefully acknowledged. T.D.F. also acknowledges the Postdoctoral Fellowship granted by NSERC.

References and Notes

- (1) Halogenic refers to the halogen and halogen-like ions such as CN⁻ and OH⁻.
- (2) DePuy, C. H.; Gronert, S.; Mullin, A.; Bierbaum, V. M. *J. Am. Chem. Soc.* **1990**, *112*, 8650.
- (3) Li, C.; Ross, P.; Szulejko, J. E.; McMahon, T. B. *J. Am. Chem. Soc.* **1996**, *118*, 9360.
- (4) Graul, S. T.; Bowers, M. T. *J. Am. Chem. Soc.* **1994**, *116*, 3875.
- (5) Angel, L. A.; Ervin, K. M. *J. Phys. Chem. A* **2001**, *105*, 4042.
- (6) LeGarrec, J.-L.; Rowe, B. R.; Queffelec, J. L.; Mitchell, J. B. A.; Clary, D. C. *J. Chem. Phys.* **1997**, *107*, 1021.
- (7) Baer, T.; Hase, W. L. In *Unimolecular Reaction Dynamics, Theory and Experiments*; Oxford: New York, 1996.
- (8) Wang, H.; Hase, W. L. *J. Am. Chem. Soc.* **1995**, *117*, 9347.
- (9) Wang, H.; Hase, W. L. *J. Am. Chem. Soc.* **1997**, *119*, 3093.
- (10) Sun, L.; Hase, W. L.; Song, K. *J. Am. Chem. Soc.* **2001**, *123*, 5753.
- (11) Su, T.; Wang, H.; Hase, W. L. *J. Phys. Chem. A* **1998**, *102*, 9819.
- (12) Wang, H.; Peshlherbe, G. H.; Hase, W. L. *J. Am. Chem. Soc.* **1994**, *116*, 9644.
- (13) Sun, L.; Song, K.; Hase, W. L.; Sena, M.; Riveros, J. M. *Int. J. Mass Spectrom.* Submitted for publication.
- (14) Fridgen, T. D.; McMahon, T. B. *J. Am. Chem. Soc.* **2001**, *123*, 3980.
- (15) Fridgen, T. D.; Keller, J. D.; McMahon, T. B. *J. Phys. Chem. A* **2001**, *105*, 3816.
- (16) Fridgen, T. D.; McMahon, T. B. *J. Phys. Chem. A* **2002**, *106*, 9648.
- (17) McCormack, J. A. D.; Mayer, P. M. *Int. J. Mass Spectrom.* **2001**, *207*, 183.
- (18) McCormack, J. A. D.; Mayer, P. M. *Int. J. Mass Spectrom.* **2001**, *207*, 195.
- (19) Ochran, R. A.; Annamalai, A.; Mayer, P. M. *J. Phys. Chem. A* **2000**, *104*, 8505.
- (20) Mayer, P. M. *J. Phys. Chem. A* **1999**, *103*, 3687.
- (21) Frisch, M. J.; Trucks, G. W.; Schlegel, H. B.; Scuseria, G. E.; Robb, M. A.; Cheeseman, J. R.; Zakrzewski, V. G.; Montgomery, J. A., Jr.; Stratmann, R. E.; Burant, J. C.; Dapprich, S.; Millam, J. M.; Daniels, A. D.; Kudin, K. N.; Strain, M. C.; Farkas, O.; Tomasi, J.; Barone, V.; Cossi, M.; Cammi, R.; Mennucci, B.; Pomelli, C.; Adamo, C.; Clifford, S.; Ochterski, J.; Petersson, G. A.; Ayala, P. Y.; Cui, Q.; Morokuma, K.; Malick, D. K.; Rabuck, A. D.; Raghavachari, K.; Foresman, J. B.; Cioslowski, J.; Ortiz, J. V.; Stefanov, B. B.; Liu, G.; Liashenko, A.; Piskorz, P.; Komaromi, I.; Gomperts, R.; Martin, R. L.; Fox, D. J.; Keith, T.; Al-Laham, M. A.; Peng, C. Y.; Nanayakkara, A.; Gonzalez, C.; Challacombe, M.; Gill, P. M. W.; Johnson, B. G.; Chen, W.; Wong, M. W.; Andres, J. L.; Head-Gordon, M.; Replogle, E. S.; Pople, J. A. *Gaussian 98*; Gaussian, Inc.: Pittsburgh, PA, 1998.
- (22) Becke, A. D. *J. Chem. Phys.* **1993**, *98*, 5648.
- (23) Curtiss, L. A.; Redfern, P. C.; Raghavachari, K.; Rassolov, V.; Pople, J. A. *J. Chem. Phys.* **1999**, *110*, 4703.
- (24) We realize that both C–O bond lengths are probably the same for protonated diethyl ether; however, density functional theory, in our experience, does not provide highly symmetric geometries.
- (25) The heavier alcohol, or the one with the greater proton affinity, is always the reactant that is protonated for the purposes of these studies since experimentally it would be difficult to observe the protonated alcohol that has the lower proton affinity in the presence of the alcohol that has the higher proton affinity.
- (26) Bouchoux, G.; Choret, N. *Rapid Commun. Mass Spectrom.* **1997**, *11*, 1799.
- (27) Raghavachari, K.; Chandrasekhar, J.; Burnier, R. C. *J. Am. Chem. Soc.* **1984**, *106*, 3124.
- (28) Abboud, J.-L. M.; Notario, R.; Bertrán, J.; Taft, R. W. *J. Am. Chem. Soc.* **1991**, *113*, 4738.
- (29) Hori, K.; Abboud, J.-L. M.; Lim, C.; Fujio, M.; Tsuno, Y. *J. Org. Chem.* **1998**, *63*, 4228.
- (30) Uggerud, E. *J. Chem. Soc., Perkin Trans.* **1999**, *2*, 1459.
- (31) Fridgen, T. D.; Parnis, J. M. *Int. J. Mass Spectrom.* **1999**, *190/191*, 181.
- (32) (a) Leffler, J. E. *Science* **1953**, *117*, 340. (b) Hammond, G. S. *J. Am. Chem. Soc.* **1955**, *77*, 334.
- (33) Maksić, Z. B.; Eckert-Maksić, M.; Knežević, J. *J. Phys. Chem. A* **1998**, *102*, 1291.
- (34) McMahon, T. B.; Heinis, T.; Nicol, G.; Hovey, J. K.; Kebarle, P. *J. Am. Chem. Soc.* **1988**, *110*, 7591.
- (35) Fridgen, T. D.; McMahon, T. B. *J. Phys. Chem. A* **2002**, *106*, 1576.